Title: Reducing adverse impacts of Amazon hydropower expansion on people and nature

Authors: Alexander S. Flecker[1*], Qinru Shi[2], Rafael M. Almeida[1,3], Héctor Angarita[4], Jonathan M. Gomes-Selman[5], Roosevelt García-Villacorta[1,6], Suresh A. Sethi[3], Steven A. Thomas[7], N. LeRoy Poff[8,9], Bruce R. Forsberg[10,11], Sebastian A. Heilpern[3,12], Stephen K. Hamilton[13,14], Jorge D. Abad[15], Elizabeth P. Anderson[16], Nathan Barros[17], Isabel Carolina Bernal[18], Richard Bernstein[2], Carlos M. Cañas[19], Olivier Dangles[20], Andrea C. Encalada[21], Ayan S. Fleischmann[22], Michael Goulding[23], Jonathan Higgins[24], Céline Jezequel[25], Erin I. Larson[1,26], Peter B. McIntyre[3], John M. Melack[27], Mariana Montoya[19], Thierry Oberdorff[25], Rodrigo Paiva[22], Guillaume Perez[2], Brendan H. Rappazzo[2], Scott Steinschneider[28], Sandra Torres[29,30], Mariana Varese[19], M. Todd Walter[28], Xiaojian Wu[2], Yexiang Xue[2,31], Xavier E. Zapata-Ríos[29,30], and Carla P. Gomes[2*]

Affiliations:
[1]Department of Ecology and Evolutionary Biology, Cornell University, Ithaca, NY 14853, USA
[2]Institute for Computational Sustainability, Cornell University, Ithaca, NY 14853, USA
[3]Department of Natural Resources and the Environment, Cornell University, Ithaca, NY 14853, USA
[4]Stockholm Environment Institute Latin America, Bogota, 110231, Colombia
[5]Department of Computer Science, Stanford University, Palo Alto, CA 94305, USA
[6] Centro Peruano para la Biodiversidad y Conservación (PCBC), Iquitos, Perú
[7]School of Natural Resources, University of Nebraska, Lincoln, NE 68583, USA
[8]Department of Biology, Colorado State University, Fort Collins, CO 80526, USA
[9]Institute for Applied Ecology, University of Canberra, ACT 2617, Australia
[10]National Institute of Amazonian Research (INPA), Manaus, 69060-001, Brazil
[11]Vermont Department of Environmental Conservation, Montpelier, VT, USA
[12]Department of Ecology, Evolution and Environmental Biology, Columbia University, New York, NY, USA
[13]Michigan State University, W.K. Kellogg Biological Station and Department of Integrative Biology, Hickory Corners, MI, 49060, USA
[14]Cary Institute of Ecosystem Studies, Millbrook, NY, 12545, USA
[15]Centro de Investigación y Tecnología del Agua (CITA), Universidad de Ingeniería y Tecnología, Lima 15063, Peru
[16]Department of Earth and Environment, Florida International University, Miami, FL 33199, USA
[17]Department of Biology, Federal University of Juiz de Fora, Juiz de Fora, 36036-900, Brazil
[18]Departamento de Geología, Escuela Politecnica Nacional, Quito, Ecuador
[19]Wildlife Conservation Society Peru, Lima, 15048, Peru
[20]Centre d'Ecologie Fonctionnelle et Evolutive, Université de Montpellier, UMR 5175, CNRS, Université Paul Valéry Montpellier, EPHE, IRD, Montpellier, France
[21]Instituto BIOSFERA, Laboratorio de Ecología Acuática, Universidad San Francisco de Quito, Quito, Ecuador
[22]Institute of Hydraulic Research, Federal University of Rio Grande do Sul, Porto Alegre, Brazil

[23]Wildlife Conservation Society, New York, NY, USA
[24]The Nature Conservancy (TNC), Chicago, IL, USA
[25]UMR EDB (Laboratoire Évolution et Diversité Biologique), CNRS 5174, IRD253, UPS; 118 route de Narbonne, F-31062 Toulouse, France
[26]Institute for Culture and Environment, Alaska Pacific University, Anchorage, AK, 99508, USA
[27]Bren School of Environmental Science and Management, University of California at Santa Barbara, Santa Barbara, CA, 93106 USA
[28]Department of Biological and Environmental Engineering, Cornell University, Ithaca, NY 14853, USA
[29]Departamento de Ingeniería Civil y Ambiental, Escuela Politécnica Nacional. Quito, Ecuador
[30]Centro de Investigaciones y Estudios en Recursos Hídricos (CIERHI), Escuela Politécnica Nacional, Quito, Ecuador
[31]Department of Computer Science, Purdue University, West Lafayette, IN, USA

*Corresponding author. Email: asf3@cornell.edu
*Corresponding author. Email: gomes@cs.cornell.edu

Abstract: Proposed hydropower dams at over 350 sites throughout the Amazon require strategic evaluation of tradeoffs with the numerous ecosystem services provided by Earth's largest and most biodiverse river basin. These services are spatially variable, hence the configuration of dams determines their collective impact. We use multi-objective optimization to identify portfolios of sites that simultaneously minimize impacts on river connectivity, sediment transport, river flow, greenhouse gas emissions, and fish diversity while achieving energy production goals. We find that uncoordinated, dam-by-dam hydropower expansion to date has resulted in foregone ecosystem service benefits. Minimizing further damage from hydropower development requires considering diverse environmental impacts across the entire basin, as well as cooperation among Amazonian nations. Our findings offer a model for rigorous assessment of hydropower expansion in transboundary basins around the world.

One Sentence Summary: Computational advances reveal opportunities for more sustainable hydropower development in large transboundary river basins

Main Text:

Hydropower is a leading component of current and future renewable energy portfolios in many countries worldwide. While the construction of new large hydropower projects has abated in much of Western Europe and North America (*1*), where coordinated dam removals are being considered (*2, 3*), construction of large dams is booming in many countries with emerging economies (*4, 5*). As plans for hydropower expansion ramp up for the world's few remaining unregulated and unfragmented river basins (*6*), tools for strategic dam planning are urgently needed (*7, 8*). Computational breakthroughs offer new opportunities to guide dam site selection based on tradeoffs among many different environmental criteria across multiple spatial scales and complex political landscapes (*9*).

From a socio-environmental perspective, hydropower proliferation is an especially acute issue in tropical river basins such as the Amazon (*10-12*). Currently, at least 158 dams with individual installed capacities (>1 MW) are operating or under construction in the five nations that constitute >90% of the Amazon Basin, and another 351 dams are proposed (Fig. 1). The distribution of existing and potential hydropower is uneven among the major sub-basins of the Amazon; most of the proposed sites are in either the Tapajós sub-basin draining the Brazilian shield in the east (144 proposed dams) or the Marañon sub-basin draining the Andes Mountains (62 proposed dams) (table S1). Amazonian dams are also getting bigger and installed on ever larger rivers (Fig. 1B), leading to more expansive inundation and greater potential for socio-environmental disruptions (*13, 14*). The variety of project sizes, combined with spatially heterogeneous river characteristics and transboundary resources, necessitates better understanding the tradeoffs between hydropower capacity and ecosystem services among different portfolios of future dams.

We developed a multi-objective optimization framework to evaluate the tradeoffs at large basin-wide scales between hydropower capacity and a set of five environmental criteria that encompass core river ecosystem services (or disservices) – river connectivity, sediment transport, degree of regulation, fish biodiversity, and greenhouse gas emissions – based on placement of dams across the entire basin. Our approach determines the Pareto-optimal frontier, which represents a set of solutions (i.e., portfolios composed of different configurations of dams) that minimize negative effects across environmental objectives for any given level of aggregate hydropower yield. This optimization problem is computationally intensive because it requires accounting for 2^{509} (10^{153}) possible combinations of the 509 current and proposed dams of the Amazon. To overcome this challenge, we developed a fully polynomial-time approximation algorithm based on dynamic programming that can quickly approximate the Pareto frontier for multiple environmental criteria simultaneously and with theoretical optimality guarantees (*15-17*), in contrast to previous heuristic approaches. Given the vast number of Pareto-optimal solutions and the limitations of human cognition to visualizing high-dimensional spaces such as a 6-dimensional Pareto frontier, we developed an interactive graphical user interface (GUI) to navigate the high-dimensional solution space for Amazon dams (Supplementary Text 1; (*18*)).

Optimization across all dam sites to achieve current levels of hydropower production shows that the historical lack of planning has produced a configuration of dams that is grossly sub-optimal from an environmental perspective. We calculated the foregone ecosystem service benefits resulting from ad-hoc dam planning by approximating separately for each environmental criterion the Pareto frontier for all existing (i.e., built and under construction) plus proposed dams for the entire Amazon Basin (>6.3 million km^2 in area) across hydropower energy capacities. Thus, we compared tradeoffs between energy and ecosystem services from the Pareto frontier that could have been achieved if optimal dam planning had been initiated from the commencement of dam building in the Amazon, to the Pareto frontier that can be achieved moving forward given the historical chronology of built dams. Criteria such as river connectivity, based on a dendritic river connectivity index (RCI_P) that quantifies drainage network fragmentation, have changed dramatically from the initial historic pre-dam baseline (Fig. 2A). River connectivity throughout the Amazon remained relatively intact until recently, with a loss of less than 10% between 1914 (when the first dam was built in the basin) and 2012. However, the blockage of major tributaries by construction of two large dams on the Madeira River – the Santo Antônio and Jirau (closed in 2012 and 2013, respectively) – as well as the Belo Monte dam on the Xingu River (closed in 2016) has led to abrupt and steep declines in river connectivity. These three recent projects, among the largest in the world, have increased fragmentation of the Amazon river network by nearly 50% in the last decade. Comparing the existing and baseline Pareto frontiers illustrates that other configurations of dams could have delivered equivalent amounts of hydropower capacity as exists today in the Amazon, with relatively little loss in connectivity (Fig. 2A). Conversely, up to four times as much hydropower capacity could have been developed through coordinated planning, if dams were selected to maximize energy production without exceeding current levels of connectivity loss. While the loss of connectivity has been rapid, other criteria, such as the degree of river flow regulation, are still close to the original Pareto frontier condition (Fig. 2), demonstrating the heterogeneous impacts of dam development among different ecosystems services.

Looking forward, the enormous differences in environmental impact per unit of electricity production illustrated by our Pareto frontier analyses underscore the need for strategic, basin-wide planning of any further hydropower expansion based on many criteria. Both computational challenges and data limitations have constrained previous basin-wide hydropower planning to include only one or a few environmental objectives at a time (*13, 19-22*). Yet rivers provide suites of ecosystem services that are potentially impacted by damming, and jointly considering multiple criteria can substantially alter optimization outcomes. In contrast to two-dimensional Pareto frontiers exploring tradeoffs only between energy production and connectivity (Fig. 3A), simultaneous consideration of additional criteria (sediment delivery, degree of regulation, fish biodiversity, greenhouse gas emissions) indeed results in dramatic changes in the identity and frequency of particular dams occurring within optimal dam portfolios. These changes in optimization outcomes ensue because tradeoffs emerge among river ecosystem services (Fig. 3A). For example, optimal solutions for river connectivity include many high-elevation dams at sites farthest away from the mouth of the Amazon; consequently, dams in the high Andes are often included in Pareto-optimal solutions when optimizing only for river connectivity (Fig. 3B). Conversely, Andean-sourced rivers produce most of the nutrient-rich sediment in the Amazon River that sustain productivity and structure the geomorphology of the floodplains (Fig. 1D); accordingly, dams in Andean-sourced rivers interrupt sediment transport more substantially and are therefore rarely contained in Pareto-optimal solutions for sediments alone (Fig. 3B). Thus, replacing one environmental criterion with another can drastically modify the frequency that some dams are Pareto optimal (Fig. 3A). Notably, about 60% of proposed Amazon dams always appear in Pareto-optimal solutions for some environmental criteria while never appearing in optimal solutions for others (Fig. 3B). Owing to this large incongruence among objectives, optimizing dam planning for a single environmental criterion inevitably results in suboptimal performance for other environmental criteria (Fig. 3C).

This case is clearly illustrated when comparing the sediment transport outcomes optimized for river connectivity compared to those attained when optimized directly for sediments (Fig. 3C). As an example, dam portfolios for 80 GW planned optimally for river connectivity would trap nearly two times more sediments basin-wide than the 80 GW dam portfolio planned optimally for sediments (Fig. 3C).

As more environmental criteria are evaluated simultaneously, we observe further complexity in optimization outcomes. Consequently, when all five of our environmental criteria are considered in a 6-dimensional Pareto frontier, few dams remain that are frequently Pareto optimal (Fig. 3A; see GUI supplement). In addition, a diversity of tradeoff outcomes among environmental criteria are revealed by the 6-dimensional Pareto frontier (Fig. 3D, GUI supplement). For example, our algorithm identifies 30 optimal solutions for a hydropower target of 80 GW, but these equivalently optimal dam portfolios can result in vastly dissimilar environmental performance for different individual criteria (Fig. 3D). Inevitably, some criteria need to be prioritized to the detriment of others given the sharp tradeoffs among environmental objectives that persist even under multidimensional optimal planning conditions. Clearly, basin-wide strategic planning needs to consider suites of multiple criteria simultaneously, recognizing that the addition of some criteria can greatly alter our perception of "high-impact" versus "low-impact" dams.

Yet another challenge in strategic hydropower planning is its potential dependence on the spatial scale of analyses. To quantify the importance of spatial scale, we conducted a set of analyses at sub-basin, regional, and whole-basin scales. We ranked all proposed dams based on the frequency with which these projects appear in at least 50% of Pareto-optimal solutions, with higher frequencies indicating less impactful environmental outcomes in aggregate. For example, when Pareto-optimal solutions are evaluated for sediment transport at the Western Amazon scale (Marañon, Napo and Ucayali sub-basins), 32% of proposed dams (36 of 114 dams) appear in at least half of the Pareto-optimal portfolios (Fig. 3E). In contrast, when optimizing for sediment transport at the scale of the entire Amazon Basin, fewer than 20% (21 of 114) of these same dams appear in at least half of the Pareto-optimal portfolios (Fig. 3E). Moreover, while about 48% of the proposed Tapajós River dams (70 of 144 dams) appear in at least half of the Pareto-optimal portfolios at the Tapajós optimization scale, nearly all of these same dams (142 of 144) are included at the whole-basin scale. The clear-water Tapajós River originates in Precambrian shields in the Eastern Amazon and is characteristically sediment-poor, whereas Western Amazon rivers drain geologically younger terrains in the Andes and are notoriously sediment-rich (*23, 24*). Consequently, Tapajós dams fare better when optimizing for sediment at larger spatial scales that include consideration of dams in sediment-rich rivers. These findings bolster the notion that planners and decision makers need to consider how spatial scale influences their perceptions of better solutions with respect to different environmental criteria.

Our results illustrate how strategic, basin-wide planning enhances the probability of selecting dam configurations with less destructive, aggregate environmental outcomes. In practice, however, hydropower planning generally occurs at the national scale, even though electricity may be exported across borders, for example from the Andean Amazon countries to Brazil. We assessed the potential of international cooperation to improve environmental outcomes by comparing basin-wide Pareto frontiers with those based on country-level optimal planning for each of our five environmental criteria. Clear opportunities exist for reducing environmental costs through international cooperation (Fig. 4). For example, developing 50% of the proposed hydropower potential optimally on a country scale but without international coordination would result in trapping about 45% more sediments on a basin-wide scale (Fig. 4A). For all Amazon countries, optimal planning at the country scale yields sub-optimal environmental outcomes at the whole-basin scale for at least one of our five environmental criteria (Fig. 4B). Further, dam sites that are disfavored in a country-scale analysis are frequently strongly favored in Amazon-wide optimization. This disparity in site prioritization between scales is especially notable for proposed dams in Ecuador. Since almost all Ecuadorian dams are run-of-river projects located in the Andes at mid to high elevations in the far western Amazon Basin, they would fragment comparatively short river segments (*25*), yield relatively small greenhouse gas emissions (*13*), and are often situated in montane zones beyond the distributional limits of diverse Amazon fish assemblages. However, our analyses only focus on ecosystem services, and do not include other factors such as seismic risk and long energy transmission distances that could make dams in Ecuador much less appealing when a broader suite of planning objectives are considered.

Conclusion and prospects

Enhanced computational tools are unlocking the potential for strategic, basin-wide planning to guide dam site selection during hydropower expansion, and our findings highlight four key principles for minimizing ecosystem service impacts in the Amazon.

First, uncoordinated hydropower planning inevitably results in environmentally more detrimental outcomes, as illustrated by the large foregone ecosystem service benefits associated with historical dam-by-dam development in the Amazon (Fig. 2). Although decision makers ideally want tools to guide decisions on which dams to build next, our approach is best suited to provide an initial filter for identifying projects that are most likely to negatively impact ecosystem services, as well as those that should be least impactful.

Second, hydropower projects influence multiple river ecosystem services and thus simultaneous consideration of multiple criteria is essential for identifying the least impactful projects (Fig. 3). While evaluating tradeoffs between hydropower and a single criterion, such as river network connectivity, can identify especially destructive projects for maintaining free-flowing rivers, this conclusion erodes when additional criteria are considered. Although we focused on five important environmental criteria as a first filter, we recognize that additional objectives (political, economic, social, environmental) should be included for overall strategic hydropower development planning (*8, 26*). Further, it will be critical to consider additional uncertainties—such as climate change, disruptions in governance, and adoption of alternative energy sources (e.g., wind, solar)— before embracing hydropower expansion in the Amazon (*27, 28*). There may well be even lower-impact paths to regional energy security.

Third, perception of which potential dam sites are high- and low-impact depends not only on the criteria being assessed, but also the spatial scale of the analysis. Optimization of dam site selection at national, sub-basin, and whole-basin scales often yields conflicting results for particular projects because the pool of candidates increases with area, and the perspective of the magnitude of impacts in any region can be modified by changing geographical scale (Figs. 3-4). This creates risk of misguided decision making, as seemingly low-impact dams based on optimization at the sub-basin or country level can in reality be highly problematic in the context of the entire basin.

Finally, international cooperation is paramount for reducing adverse impacts of hydropower expansion in transboundary basins (Fig. 4). Without a basin-wide approach to planning, a sustainable path for energy development in the Amazon will remain elusive. Coordinated planning moving forward is challenging and requires mechanisms for cooperative agreements and their enforcement. For example, the Amazon Cooperation Treaty Organization (ACTO) has existed for nearly two decades, but this transboundary policy instrument has not yet been leveraged to enhance the scale and caliber of integrated environmental assessments of Amazon hydropower (*11*). The Leticia Pact, signed in 2019, provides a fresh opportunity for a watershed approach to cooperation among Amazon countries through mutual agreements regarding sustainable Amazon development (*29*). The data and tools produced by this study can provide unbiased input to such policy instruments, but first political leaders must recognize the collective benefits of basin-wide strategic planning for hydropower expansion in any transboundary river basin.

References and Notes

1. J. E. O'Connor, J. J. Duda, G. E. Grant, 1000 dams down and counting. *Science* **348**, 496-497 (2015).
2. M. J. Kuby, W. F. Fagan, C. S. ReVelle, W. L. Graf, A multiobjective optimization model for dam removal: an example trading off salmon passage with hydropower and water storage in the Willamette basin. *Advances in Water Resources* **28**, 845-855 (2005).
3. S. G. Roy *et al.*, A multiscale approach to balance trade-offs among dam infrastructure, river restoration, and cost. *Proceedings of the National Academy of Sciences* **115**, 12069-12074 (2018).
4. K. O. Winemiller *et al.*, Balancing hydropower and biodiversity in the Amazon, Congo, and Mekong. *Science* **351**, 128-129 (2016).
5. C. Zarfl, A. Lumsdon, J. Berlekamp, L. Tydecks, K. Tockner, A global boom in hydropower dam construction. *Aquatic Sciences* **77**, 161-170 (2014).
6. G. Grill *et al.*, Mapping the world's free-flowing rivers. *Nature* **569**, 215-221 (2019).
7. J. Opperman *et al.*, "Connected and flowing: A renewable future for rivers, climate and people," (WWF and The Nature Conservancy, Washington, DC, 2019).
8. E. F. Moran, M. C. Lopez, N. Moore, N. Müller, D. W. Hyndman, Sustainable hydropower in the 21st century. *Proceedings of the National Academy of Sciences*, (2018).
9. C. Gomes *et al.*, Computational sustainability: computing for a better world and a sustainable future. *Commun. ACM* **62**, 56–65 (2019).
10. L. Castello, M. N. Macedo, Large-scale degradation of Amazonian freshwater ecosystems. *Global Change Biology* **22**, 990-1007 (2016).
11. E. M. Latrubesse *et al.*, Damming the rivers of the Amazon basin. *Nature* **546**, 363-369 (2017).
12. J. G. Tundisi, J. Goldemberg, T. Matsumura-Tundisi, A. C. F. Saraiva, How many more dams in the Amazon? *Energ Policy* **74**, 703-708 (2014).
13. R. M. Almeida *et al.*, Reducing greenhouse gas emissions of Amazon hydropower with strategic dam planning. *Nature Communications* **10**, 4281 (2019).

14. H. I. Jager, R. A. Efroymson, J. J. Opperman, M. R. Kelly, Spatial design principles for sustainable hydropower development in river basins. *Renewable and Sustainable Energy Reviews* **45**, 808-816 (2015).
15. J. M. Gomes-Selman *et al.* (Springer International Publishing, Cham, 2018), pp. 263-279.
16. Q. Shi *et al.*, paper presented at the Proceedings of the 1st ACM SIGCAS Conference on Computing and Sustainable Societies, Menlo Park and San Jose, CA, USA, 2018.
17. X. Wu *et al.*, paper presented at the AAAI, 2018.
18. https://www.cs.cornell.edu/gomes/udiscoverit/amazon-ecovistas/.
19. T. B. A. Couto, M. L. Messager, J. D. Olden, Safeguarding migratory fish via strategic planning of future small hydropower in Brazil. *Nature Sustainability*, (2021).
20. R. J. P. Schmitt, S. Bizzi, A. Castelletti, G. M. Kondolf, Improved trade-offs of hydropower and sand connectivity by strategic dam planning in the Mekong. *Nature Sustainability* **1**, 96-104 (2018).
21. R. J. P. Schmitt, S. Bizzi, A. Castelletti, J. J. Opperman, G. M. Kondolf, Planning dam portfolios for low sediment trapping shows limits for sustainable hydropower in the Mekong. *Science Advances* **5**, eaaw2175 (2019).
22. G. Ziv, E. Baran, S. Nam, I. Rodríguez-Iturbe, S. A. Levin, Trading-off fish biodiversity, food security, and hydropower in the Mekong River Basin. *Proceedings of the National Academy of Sciences* **109**, 5609-5614 (2012).
23. J. A. Constantine, T. Dunne, J. Ahmed, C. Legleiter, E. D. Lazarus, Sediment supply as a driver of river meandering and floodplain evolution in the Amazon Basin. *Nat Geosci* **7**, 899-903 (2014).
24. B. R. Forsberg *et al.*, The potential impact of new Andean dams on Amazon fluvial ecosystems. *Plos One* **12**, e0182254 (2017).
25. E. P. Anderson *et al.*, Fragmentation of Andes-to-Amazon connectivity by hydropower dams. *Science Advances* **4**, eaao1642 (2018).
26. S. Athayde *et al.*, Mapping research on hydropower and sustainability in the Brazilian Amazon: advances, gaps in knowledge and future directions. *Current Opinion in Environmental Sustainability* **37**, 50-69 (2019).
27. F. A. M. de Faria, P. Jaramillo, The future of power generation in Brazil: An analysis of alternatives to Amazonian hydropower development. *Energy for Sustainable Development* **41**, 24-35 (2017).
28. N. L. Poff *et al.*, Sustainable water management under future uncertainty with eco-engineering decision scaling. *Nat Clim Change* **6**, 25-34 (2016).
29. P. R. Prist *et al.*, Collaboration across boundaries in the Amazon. *Science* **366**, 699-700 (2019).
30. ECOA, International Rivers & Fundacion Proteger. "Dams in Amazonia", http:// dams-info.org/en (2018).
31. Agência Nacional de Energia Elétrica (ANEEL, Brasil). "Inventários Hidrelétricos", http://www.aneel.gov.br/inventario-hidreletricos (2018).
32. Ministerio de Electricidad y Energía Renovable (Ecuador), "Plan maestro de electricidad 2016-2025," (Quito, 2017).
33. B. Lehner *et al.*, Global Reservoir and Dam Database, Version 1 (GRanDv1): Dams, Revision 01. (2011).
34. X. Wu, D. Sheldon, S. Zilberstein, in *Proceedings of the 28th AAAI Conference on Artificial Intelligence (AAAI)*. (2014), pp. 479-485.

35. X. Wu, D. Sheldon, S. Zilberstein, in *Advances in Neural Information Processing Systems (NIPS)*. (2014), pp. 892-890.
36. M. Goulding *et al.*, Ecosystem-based management of Amazon fisheries and wetlands. **20**, 138-158 (2019).
37. D. Cote, D. G. Kehler, C. Bourne, Y. F. Wiersma, A new measure of longitudinal connectivity for stream networks. *Landscape Ecology* **24**, 101-113 (2009).
38. G. Grill, C. Ouellet Dallaire, E. Fluet Chouinard, N. Sindorf, B. Lehner, Development of new indicators to evaluate river fragmentation and flow regulation at large scales: A case study for the Mekong River Basin. *Ecological Indicators* **45**, 148-159 (2014).
39. J. A. Downing *et al.*, Global abundance and size distribution of streams and rivers. *Inland Waters* **2**, 229-236 (2012).
40. C. Jézéquel *et al.*, Freshwater fish diversity hotspots for conservation priorities in the Amazon Basin. *Conserv Biol* **34**, 956-965 (2020).
41. M. D. Crisp, S. Laffan, H. P. Linder, A. Monro, Endemism in the Australian flora. *Journal of Biogeography* **28**, 183-198 (2001).
42. T. Oberdoff, J.-F. Guégan, B. Hugueny, Global scale patterns of fish species richness in rivers. *Ecography* **18**, 345-352 (1995).
43. M. A. Xenopoulos, D. M. Lodge, Going with the flow: Using species-discharge relationships to forecast losses in fish biodiversity. *Ecology* **87**, 1907-1914 (2006).
44. S. E. Bunn, A. H. Arthington, Basic Principles and Ecological Consequences of Altered Flow Regimes for Aquatic Biodiversity. *Environ Manage* **30**, 492-507 (2002).
45. N. L. Poff, J. D. Olden, D. M. Merritt, D. M. Pepin, Homogenization of regional river dynamics by dams and global biodiversity implications. *Proceedings of the National Academy of Sciences* **104**, 5732-5737 (2007).
46. K. Timpe, D. Kaplan, The changing hydrology of a dammed Amazon. *Science Advances* **3**, e1700611 (2017).
47. G. Grill *et al.*, An index-based framework for assessing patterns and trends in river fragmentation and flow regulation by global dams at multiple scales. *Environ Res Lett* **10**, 015001 (2015).
48. B. Lehner *et al.*, High-resolution mapping of the world's reservoirs and dams for sustainable river-flow management. *Front Ecol Environ* **9**, 494-502 (2011).
49. H. E. Beck *et al.*, MSWEP: 3-hourly 0.25° global gridded precipitation (1979–2015) by merging gauge, satellite, and reanalysis data. *Hydrol. Earth Syst. Sci.* **21**, 589-615 (2017).
50. T. Dunne, L. A. K. Mertes, R. H. Meade, J. E. Richey, B. R. Forsberg, Exchanges of sediment between the flood plain and channel of the Amazon River in Brazil. *Geol Soc Am Bull* **110**, 450-467 (1998).
51. E. Wohl *et al.*, The Natural Sediment Regime in Rivers: Broadening the Foundation for Ecosystem Management. *Bioscience* **65**, 358-371 (2015).
52. J. P. M. Syvitski *et al.*, Sinking deltas due to human activities. *Nature Geosci* **2**, 681-686 (2009).
53. G. E. Grant, J. C. Schmidt, S. L. Lewis, in *A Peculiar River,* J. E. O'Connor, G. E. Grant, Eds. (2003), pp. 203-219.
54. T. Maavara *et al.*, Global phosphorus retention by river damming. *Proc. Natl Acad. Sci.* **112**, 15603-15608 (2015).
55. G. M. Brune, Trap efficiency of reservoirs. *Eos Trans. AGU* **34**, 407-418 (1953).

56. L. L. Hess *et al.*, LBA-ECO LC-07 Wetland Extent, Vegetation, and Inundation: Lowland Amazon Basin. ORNL DAAC, Oak Ridge, Tennessee, USA. (2015).
57. B. R. Deemer *et al.*, Greenhouse Gas Emissions from Reservoir Water Surfaces: A New Global Synthesis. *Bioscience* **66**, 949-964 (2016).
58. Y. T. Prairie *et al.*, Greenhouse gas emissions from freshwater reservoirs: What does the atmosphere see? *Ecosystems*, (2017).
59. F. A. M. de Faria, P. Jaramillo, H. O. Sawakuchi, J. E. Richey, N. Barros, Estimating greenhouse gas emissions from future Amazonian hydroelectric reservoirs. *Environ Res Lett* **10**, (2015).
60. M. Demarty, J. Bastien, GHG emissions from hydroelectric reservoirs in tropical and equatorial regions: Review of 20 years of CH(4) emission measurements. *Energ Policy* **39**, 4197-4206 (2011).
61. E. G. Hertwich, Addressing biogenic greenhouse gas emissions from hydropower in LCA. *Environmental Science & Technology* **47**, 9604-9611 (2013).
62. G. Myhre *et al.*, "Anthropogenic and natural radiative forcing," *Climate Change 2013: The Physical Science Basis. Contribution of Working Group I to the Fifth Assessment Report of the Intergovernmental Panel on Climate Change* (Cambridge, UK and New York, USA, 2013).
63. V. A. Siqueira *et al.*, Toward continental hydrologic–hydrodynamic modeling in South America. *Hydrol. Earth Syst. Sci.* **22**, 4815-4842 (2018).
64. E. Armijos *et al.*, Yields of suspended sediment and dissolved solids from the Andean basins of Ecuador. *Hydrological Sciences Journal* **58**, 1478-1494 (2013).
65. M. T. Coe, M. H. Costa, E. A. Howard, Simulating the surface waters of the Amazon River basin: impacts of new river geomorphic and flow parameterizations. *Hydrological Processes* **22**, 2542-2553 (2008).
66. A. Laraque, J. Ronchail, G. Cochonneau, R. Pombosa, J. L. Guyot, Heterogeneous Distribution of Rainfall and Discharge Regimes in the Ecuadorian Amazon Basin. *Journal of Hydrometeorology* **8**, 1364-1381 (2007).
67. J.-S. Moquet *et al.*, Chemical weathering and atmospheric/soil CO2 uptake in the Andean and Foreland Amazon basins. *Chemical Geology* **287**, 1-26 (2011).
68. A. Ovando *et al.*, Extreme flood events in the Bolivian Amazon wetlands. *Journal of Hydrology: Regional Studies* **5**, 293-308 (2016).
69. E. Pepin *et al.*, Climatic control on eastern Andean denudation rates (Central Cordillera from Ecuador to Bolivia). *J S Am Earth Sci* **44**, 85-93 (2013).
70. J. M. Tucker Lima *et al.*, A social-ecological database to advance research on infrastructure development impacts in the Brazilian Amazon. *Scientific Data* **3**, 160071 (2016).
71. P. Vauchel *et al.*, A reassessment of the suspended sediment load in the Madeira River basin from the Andes of Peru and Bolivia to the Amazon River in Brazil, based on 10years of data from the HYBAM monitoring programme. *Journal of Hydrology* **553**, 35-48 (2017).

Acknowledgments: This work was carried out by our Amazon Dams Computational Sustainability Working Group based at Cornell University. We thank the Cornell Atkinson Center, the Universidad de Ingeniería y Tecnología (UTEC) in Lima, Peru, and Florida International University for hosting working group meetings to develop the project framework.

The Amazon Fish Project (https://www.amazon-fish.com/) provided data for fish biodiversity threat analyses. We want to acknowledge the inspirational ideas of our late colleagues Dr. Greg Poe and Dr. Javier Maldonado-Ocampo, who were instrumental in the conceptualization of this work.

Funding: This work was funded by an NSF Expeditions in Computing award (CCF-1522054) to CPG and a Cornell University Atkinson Academic Venture Fund award to A.S.F., C.P.G., and S.S. Computations were performed using the AI for Discovery Avatar (AIDA) computer cluster funded by an Army Research Office (ARO), Defense University Research Instrumentation Program (DURIP) award (W911NF-17-1-0187) to CPG.

Author contributions: Conceptualization: All authors contributed to conceptualization through active participation in working group meetings. R.G.-V., Q.S., R.M.A., B.R.F., E.P.A., and A.S.F. compiled and curated the hydropower dam dataset. Hydrological and sediment flux analyses were developed by H.A., A.S.Flei., R.P., B.R.F., Q.S., S.S., N.L.P., S.A.T., S.K.H, R.M.A., R.G.-V., J.D.A., I.C.B., X.E.Z.R., S.T., and M.T.W., and were conducted by H.A., Q.S., and A.S.Flei. Dendritic connectivity was analyzed by Q.S. and R.G.-V., with assistance from S.A.S., E.P.A., C.M.C., and M.G. Fish biodiversity threat analyses were conducted by Q.S., E.I.L., and C.J. with assistance from E.P.A., C.M.C., A.C.E., J.H., M.G., O.D., M.M., and M.V., using Amazon fish data provided by T.O. Greenhouse gas emissions were analyzed by R.M.A., S.A.S. and N.B. with input from B.R.F., S.K.H., and J.M.M. Computational analyses were developed and performed by C.P.G., J.M.G.-S., Q.S., X.W., Y.X., and G.P. The interactive visual supplement (Amazon EcoVistas) was developed by R.B. and B.H.R. with input from C.P.G., Q.S., R.M.A. and S.A.H. Visualizations were made by Q.S., R.M.A., R.B., B.H.R., with significant contributions of S.A.T. and S.A.H. Funding for our Amazon Dams Computational Sustainability Working Group was acquired by C.P.G. and A.S.F. The manuscript was drafted by A.S.F., R.M.A., S.A.H., B.R.F., Q.S., C.P.G. in close collaboration with S.A.S., S.A.T., N.L.P., S.K.H., J.H., P.B.M., M.G., J.M.M., and A.S.Flei, and all authors reviewed the manuscript.

Competing interests: The authors declare that they have no competing interests.

Data and materials availability: The Pareto optimization code can be downloaded from Cornell University's Institute for Computational Sustainability url (confidential prior to publication, do not distribute, publicly available after acceptance): https://www.cs.cornell.edu/gomes/udiscoverit/amazon-pareto-frontier-review.php . The Amazon EcoVistas tutorial and visualization of the Pareto frontier is available at the url (confidential prior to publication, do not distribute; publicly available after acceptance): https://www.cs.cornell.edu/gomes/udiscoverit/amazon-ecovistas/. All relevant data are publicly available in the supplementary materials and online data repositories, or are available from the authors.

Supplementary Materials

Materials and Methods

Supplementary Text 1

Supplementary Text 2

Figs. S1 to S5

Tables S1 to S2

References (30-71)

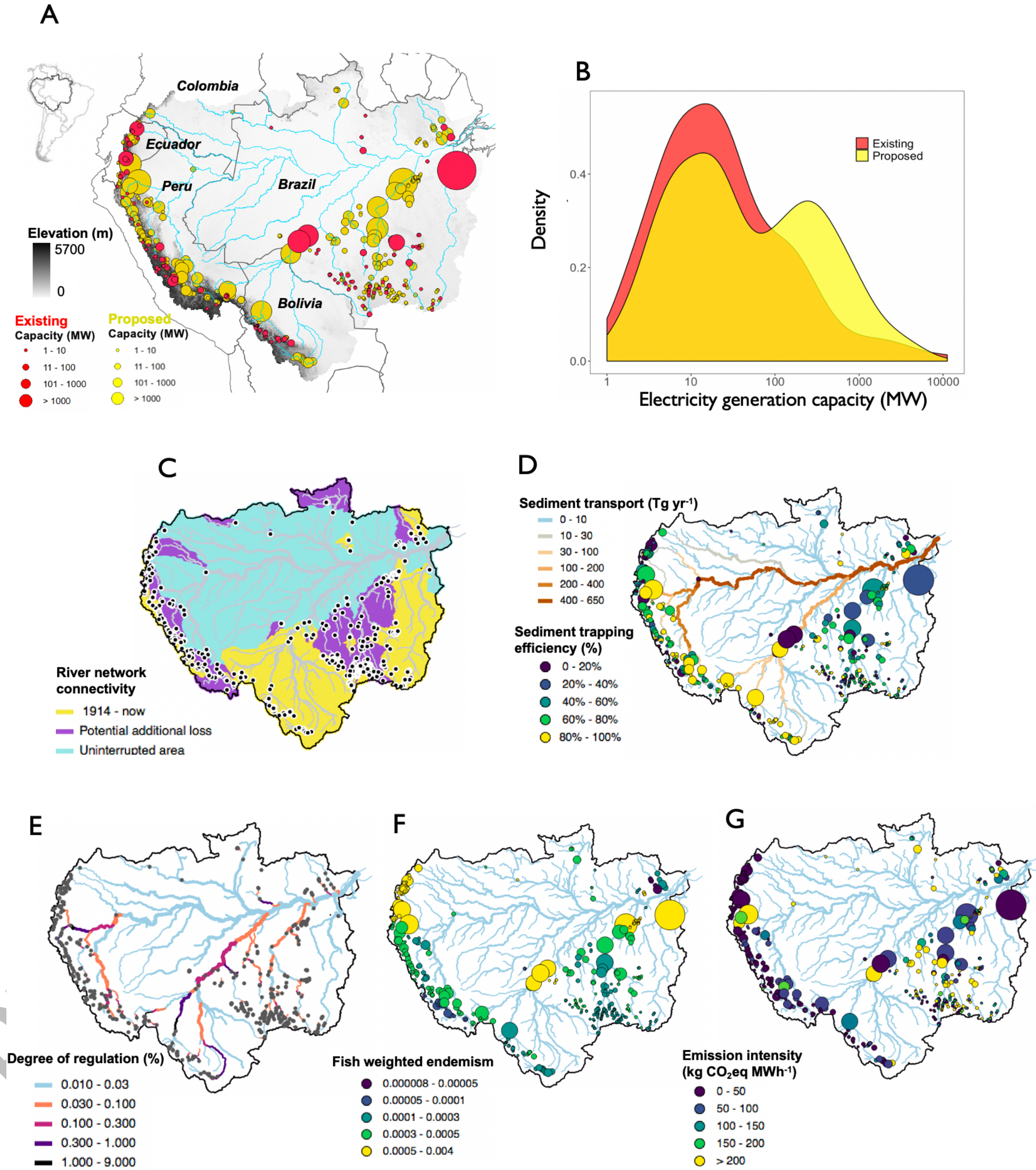

Fig. 1. Expansion of Amazon hydropower and comparative impacts for different environmental criteria. (**A**) Spatial distribution of 158 hydropower dams currently existing in the Amazon Basin and of 351 additional proposed dams. (**B**) Comparison of frequency

distributions of existing and proposed dams as a function of installed capacity shows that dams are getting bigger in the Amazon, with more projects proposed on large tributaries. The magnitude of impacts varies for different environmental criteria in different parts of the basin, as illustrated in **C-G**. (**C**) Existing dams have disconnected large fractions (~25%) of southern and western Amazon (yellow areas) as indicated by a river network connectivity index (RCI_D). Building all proposed dams would further break the Amazon Basin connectivity by ~20% (purple areas), with only about half of the basin remaining unfragmented (cyan areas). (**D**) Many dams with high sediment trapping efficiencies are proposed in sediment-rich river reaches in the western Amazon. (**E**) Cumulative degree of regulation, estimated as the percent annual flow that is withheld by upstream reservoirs with full buildout of all existing and proposed dams, can be manifested far downstream and varies across the river network. (**F**) Some dams are located in sub-basins that are fish biodiversity hotspots as indicated by weighted endemism, which incorporates both fish species richness and endemism. (**G**) Estimated greenhouse gas emissions per unit electricity generated at 351 proposed Amazon dams varies by over two orders of magnitude.

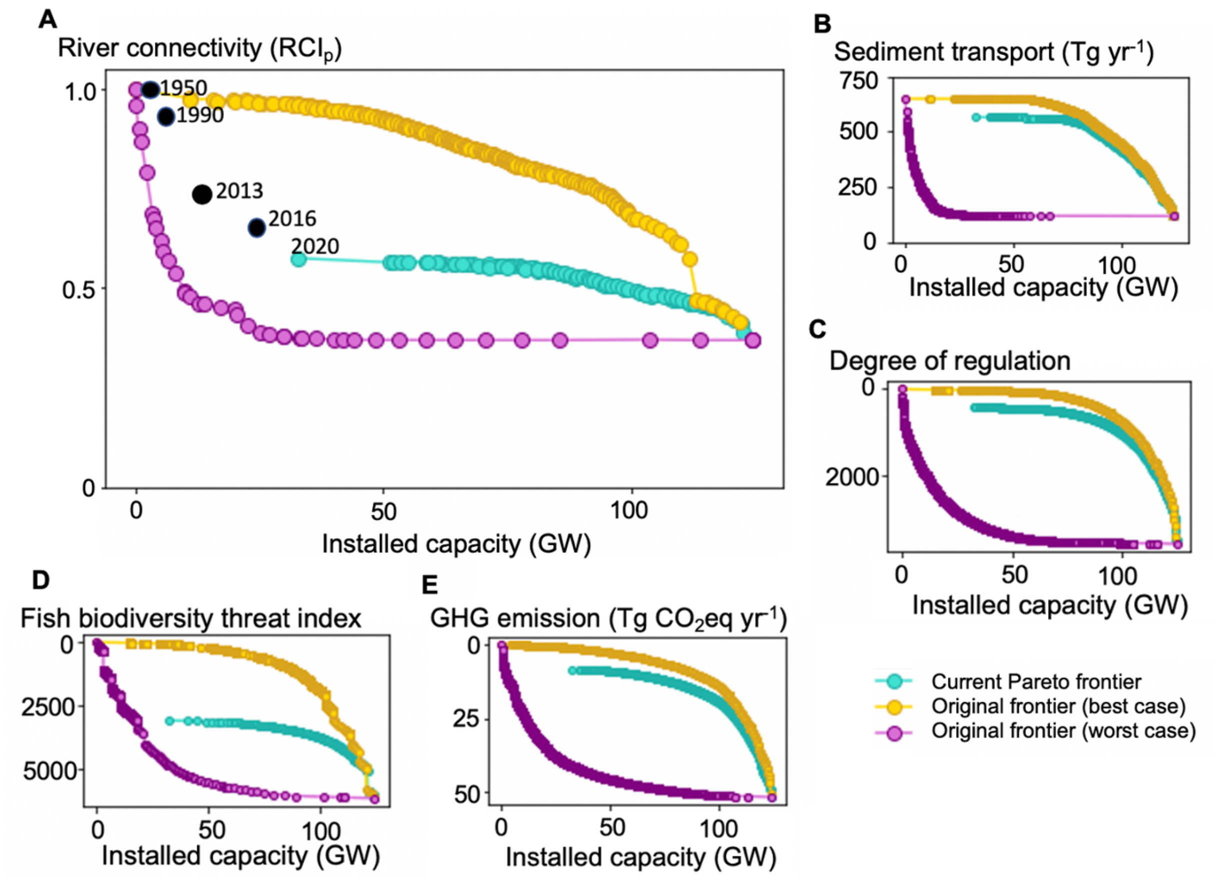

Fig. 2. Foregone environmental and energy benefits of uncoordinated dam planning in the Amazon. Pareto-optimal solutions for Amazon hydropower development based on electricity generation and different environmental criteria. For each environmental criterion (**A-E**), the plots show the original best-case scenario that could have been achieved with optimal planning from the commencement of dam building in the Amazon (yellow) compared to the original worst-case scenario (purple) for hydropower placement; black filled circles show the chronological trajectory of existing dams, whereas the cyan line shows the current possible best-case scenario for optimal hydropower placement moving forward from current conditions in 2020 for proposed dams considering (**A**) river connectivity, (**B**) sediment transport, (**C**) cumulative downstream flow alteration estimated using a degree of regulation index (values are the sum of degree of regulation for each dam portfolio), (**D**) fish biodiversity threat score, and (**E**) greenhouse gas emissions from reservoirs.

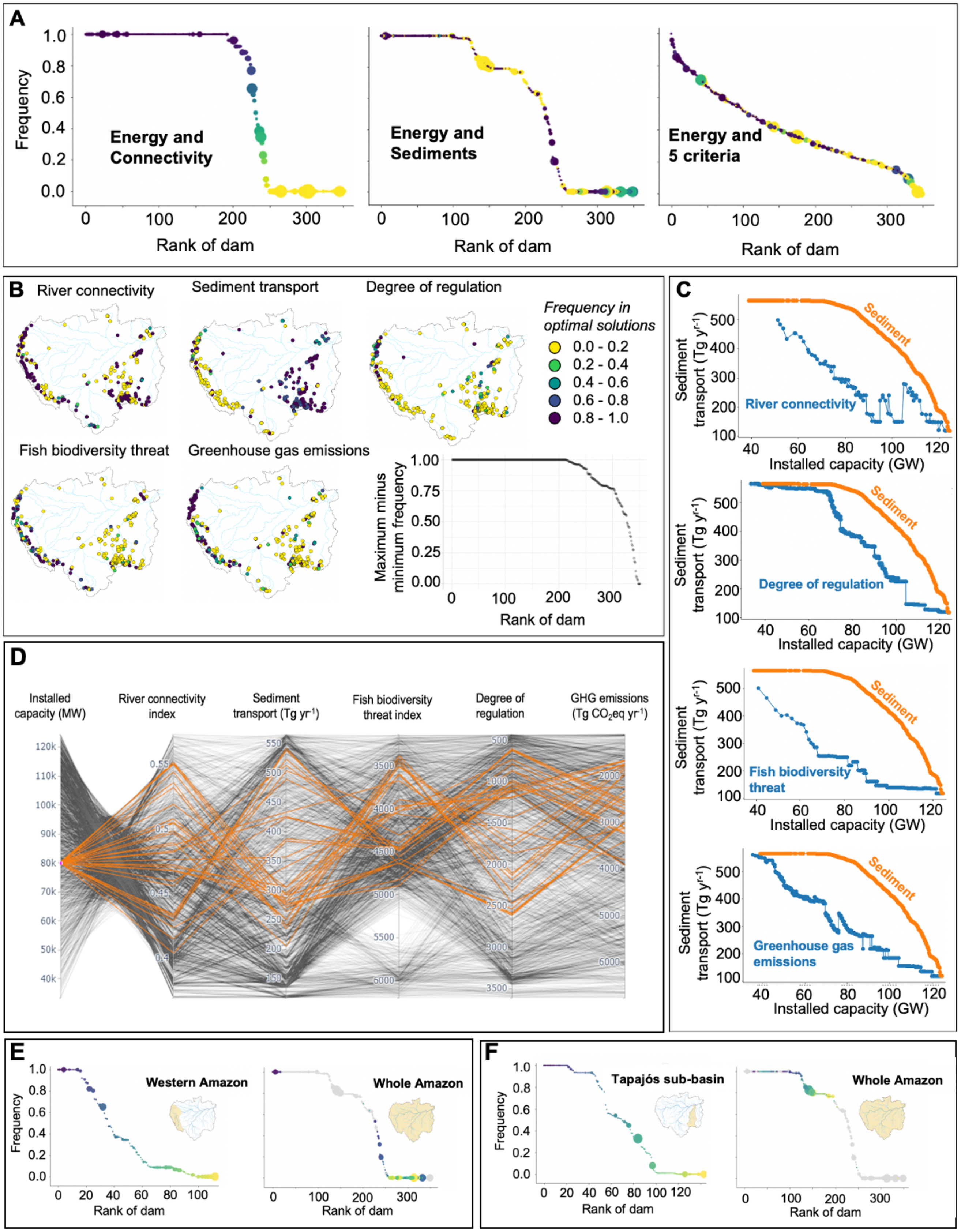
A
Energy and Connectivity
Energy and Sediments
Energy and 5 criteria
Frequency
Rank of dam
B
River connectivity
Sediment transport
Degree of regulation
Frequency in optimal solutions
0.0 - 0.2
0.2 - 0.4
0.4 - 0.6
0.6 - 0.8
0.8 - 1.0
Fish biodiversity threat
Greenhouse gas emissions
Maximum minus minimum frequency
Rank of dam
C
Sediment transport (Tg yr-1)
Installed capacity (GW)
Sediment
River connectivity
Degree of regulation
Fish biodiversity threat
Greenhouse gas emissions
D
Installed capacity (MW)
River connectivity index
Sediment transport (Tg yr-1)
Fish biodiversity threat index
Degree of regulation
GHG emissions (Tg CO2eq yr-1)
E
Western Amazon
Whole Amazon
Frequency
Rank of dam
F
Tapajós sub-basin
Whole Amazon
Frequency
Rank of dam

Fig. 3. The importance of choice of criteria and spatial scale for strategic hydropower planning. (**A**) Rank frequency plot with the frequency that each of the 351 proposed Amazon dam appears in optimal solutions for tradeoff analyses between energy and river network connectivity, sediment transport, and five environmental criteria considered simultaneously; dams in the center and right-side plot are colored according to their frequency in optimal solutions (purple = high frequency; yellow = low frequency) compared to when only energy and connectivity are analyzed (i.e., left-side plot), and dot sizes are proportional to installed capacity. (**B**) Maps showing the frequency that each dam appears in optimal solutions for each environmental criteria when they are optimized individually; the inset plot on the bottom right shows the difference between the maximum and minimum frequency in optimal solutions among the five criteria for each dam, with the 351 dams being ranked from those with higher to lower values. (**C**) Basin-wide sediment transport outcomes of Amazon dam portfolios planned optimally to minimize sediment retention in comparison to sediment outcomes attained when optimizing individually for each of the other four criteria (river connectivity, degree of regulation, fish biodiversity, and greenhouse gases). (**D**) Parallel coordinate plot with solutions that are Pareto-optimal for all criteria simultaneously. Each coordinate corresponds to a criterion, and each line connecting different values along the coordinates corresponds to a single Pareto-optimal solution; all optimal solutions for 80 ± 0.5 GW are highlighted in orange. (**E**) Rank frequency plot with the frequency that proposed dams in three Western Amazon sub-basins (Marañon, Napo, Ucayali rivers) are in configurations along the Pareto optimal frontier (left-side plot) compared to the frequency that the same proposed Western Amazon dams are in optimal solutions when analyzed at the scale of the entire Amazon basin (right-side plot); dams are colored according to their frequency in optimal solutions at the Western Amazon scale. (**F**) same as E, but for the Tapajós sub-basin. Note contrasting effects of increasing spatial scale of analysis for Western Amazon sub-basins with high sediment loads as opposed to the Tapajós sub-basin with little sediment load.

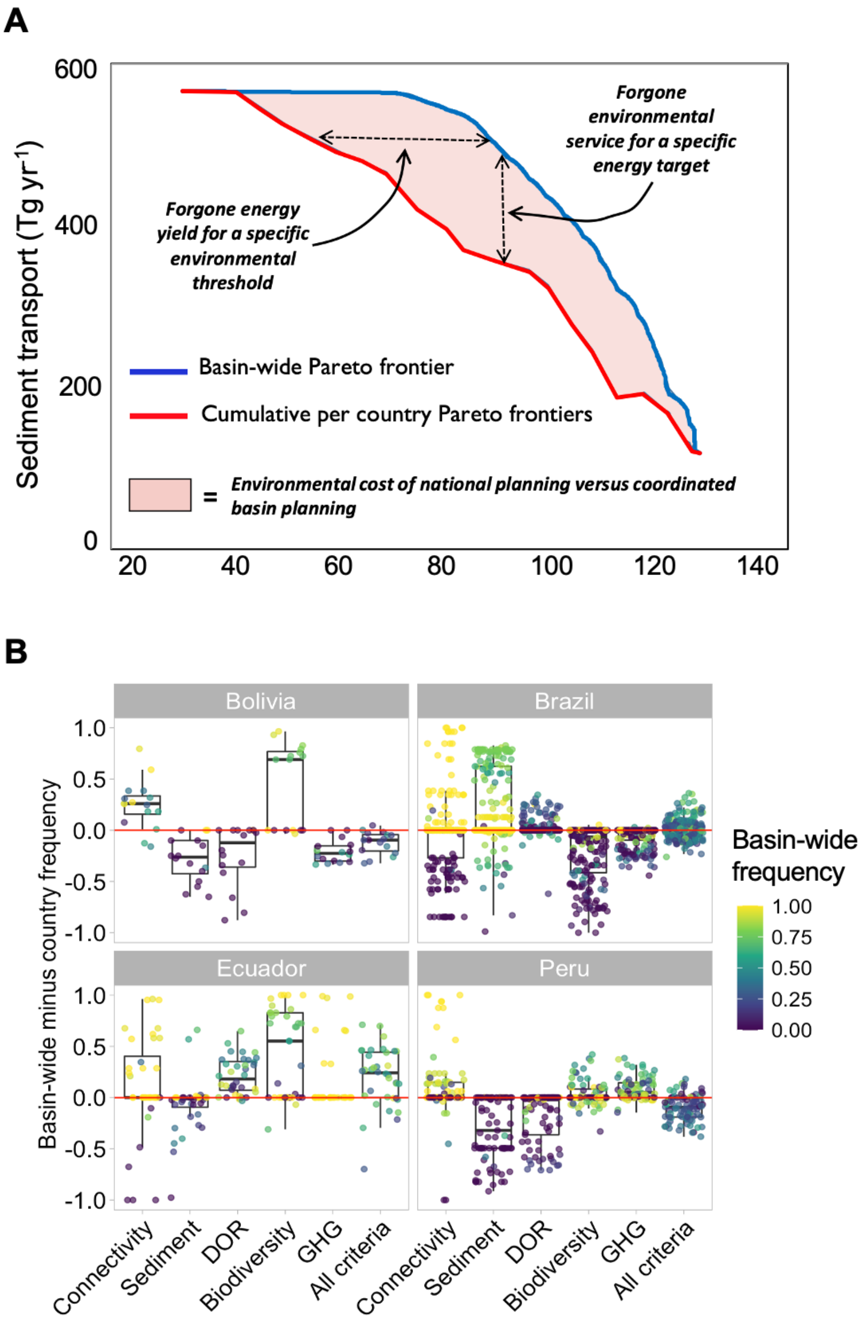

Fig. 4. International cooperation among Amazon countries can lead to more efficient strategic hydropower planning outcomes. (**A**) Pareto frontiers for cumulative country-level (red line) and basin-wide (blue-line) optimizations for sediment transport. For country-wide analyses, each country contributes an equivalent proportion of their own proposed hydropower potential towards meeting basin-level energy generation targets. The difference between basin-wide and country-level lines illustrates the environmental and hydropower costs of the lack of basin-wide strategic planning. (**B**) Disparities in the frequency that individual dams appear in optimal solutions when optimizations are run at the country versus whole-basin scales. Box and

whisker plots are shown for five environmental criteria run for four Amazon countries (Bolivia, Brazil, Ecuador, Peru) that comprise >90% of the Amazon Basin. Color gradient indicates the frequency a dam is in optimal solutions at the whole-basin scale. Positive values indicate that projects often perceived suboptimal at the country scale are less impactful than they appear when considering the broader constellation of proposed dam options across the entire Amazon Basin. Conversely, negative values indicate that projects often deemed optimal by countries are likely to be more environmentally disruptive from the perspective of the basin-wide scale, thus revealing the environmental cost of a lack of international coordination. DOR = degree of regulation; GHG = greenhouse gas emissions.

Science
AAAS

Supplementary Materials for

Reducing adverse impacts of Amazon hydropower expansion on people and nature

Alexander S. Flecker[1*], Qinru Shi[2], Rafael M. Almeida[1,3], Héctor Angarita[4], Jonathan M. Gomes-Selman[5], Roosevelt García-Villacorta[1,6], Suresh A. Sethi[3], Steven A. Thomas[7], N. LeRoy Poff[8,9], Bruce R. Forsberg[10,11], Sebastian A. Heilpern[3,12], Stephen K. Hamilton[13,14], Jorge D. Abad[15], Elizabeth P. Anderson[16], Nathan Barros[17], Isabel Carolina Bernal[18], Richard Bernstein[2], Carlos M. Cañas[19], Olivier Dangles[20], Andrea C. Encalada[21], Ayan S. Fleischmann[22], Michael Goulding[23], Jonathan Higgins[24], Céline Jezequel[25], Erin I. Larson[1, 26], Peter B. McIntyre[3], John M. Melack[27], Mariana Montoya[19], Thierry Oberdorff[25], Rodrigo Paiva[22], Guillaume Perez[2], Brendan H. Rappazzo[2], Scott Steinschneider[28], Sandra Torres[29,30], Mariana Varese[19], M. Todd Walter[28], Xiaojian Wu[2], Yexiang Xue[2,31], Xavier E. Zapata-Ríos[29,30], and Carla P. Gomes[2*]

Correspondence to: asf3@cornell.edu; gomes@cs.cornell.edu

This PDF file includes:

Materials and Methods

Supplementary Text 1

Supplementary Text 2

Figs. S1 to S5

Tables S1 to S2

Material and Methods

1. Dams database

Existing and proposed dam locations and technical information (i.e., installed capacity, reservoir surface area, reservoir volume, dam height) were obtained from published datasets (*25, 30*) and updated using recent national government databases when available (*31, 32*). The proposed dams in our database are in different stages of inventory, planning, and licensing—these stages change frequently and are subject to technical, financial, business and political drivers. Missing reservoir surface areas were estimated using a multiple regression model with country, watershed area, installed capacity and elevation as covariates (*13*). Missing reservoir volumes were estimated using empirical equations that utilize dam height and reservoir surface area as covariates (*33*). Watershed areas above each dam were estimated using a digital elevation model.

2. Multi-criteria optimization

We conducted multi-objective optimizations to minimize environmental impacts as Amazon hydropower expands through the development of novel exact dynamic-programming algorithms and fully polynomial time approximation schemes for computing the Pareto frontier for tree-structured networks. The Pareto frontier captures the tradeoffs between environmental and energy benefits, defining a set of solutions that minimize environmental disruption while satisfying varying hydropower generation goals. Our algorithms are general and can be applied to other river networks and related tree-structured network problems. We also developed an interactive graphic that helps visualize complex tradeoffs among multiple criteria across different geographic scales (*18*). Our framework contributes to the advancement of value-aligned Artificial Intelligence systems in which the objectives are consistent with human values. We provide details about the algorithms and the accompanying visualization graphics below.

2.1. Abstracting the river network into a smaller tree-structured network

The Amazon river network contains more than 3 million river segments, creating a substantial computational challenge. We first abstract the river network into a more compact tree-structured network. In this abstraction, each contiguous section of the river network uninterrupted by existing or proposed dams is represented as a node, whereas each existing or potential proposed dam location is represented by an edge directed from downstream to upstream (fig. S1) (*17*). Accordingly, the number of edges in the new tree-structured network is reduced to 509 – the number of existing and proposed dams combined.

2.2. Pareto-optimal frontier and ε-approximation.

A Pareto-optimal solution is a solution that is not dominated by any other solution, and the Pareto frontier is the set of all Pareto-optimal solutions. We define a solution π (also referred to as a portfolio) as a subset of proposed dams that could potentially be built in the Amazon. For a total of *d* objectives, we denote their values as: $z^1(\pi)$, $z^2(\pi)$, … , $z^d(\pi)$. In the following example, we assume that all objectives are non-negative and are to be maximized, but objective functions that are to be minimized (e.g. greenhouse gas emissions, fish biodiversity threat, and degree of regulation) can be treated similarly. Given two solutions π and π ', if for every objective i, $z^i(\pi) \geq$

$z^i(\pi')$ and the strict inequality holds for at least one objective, we consider that solution π dominates π'. In other words, for the example of sediment transport, if two solutions provide 30 GW of installed capacity, but solution A traps more sediment than solution B, then solution B dominates solution A because sediment trapping is considered an undesirable impact of damming.

Computing the full Pareto frontier for a multi-objective optimization problem is a non-deterministic polynomial-time hard (NP-hard) problem, meaning that the runtime could be exponential in the number of dams in the worst case. Given the large number of proposed (n = 351) and existing (n=158) Amazon dams (n=509 total) and possible dam combinations (2^{509}, or 10^{153}), computing the exact Pareto frontier for multiple criteria is intractable. Thus, our algorithm finds a set of solutions that approximate the Pareto frontier. Given two solutions π and π', we say that π ε-dominates π', if and only if, $(1+\varepsilon)\, z^i(\pi) \geq z^i(\pi')$ for every objective i. For a Pareto-optimal frontier P and a solution set P', we say that P' ε-approximates P, if and only if, for every Pareto-optimal solution $\pi \in P$, there exists a solution $\pi' \in P'$ such that π' ε-dominates π. Finding an ε-approximation of a Pareto-optimal frontier can be solved in polynomial time, and we developed an efficient algorithm for it as shown in the next section.

2.3. Dynamic-programming based approximation algorithm

We developed a fully polynomial-time approximation algorithm (FPTAS) based on Dynamic Programming (DP) that can quickly approximate the Pareto frontier for multiple criteria for any error bound $\varepsilon > 0$ (*17*). The algorithm exploits the tree-structure of the problem and recursively computes the approximate Pareto frontier above each node from leaf to root. The key insight of the algorithm is that for most of our objectives, we only need to keep the Pareto-optimal partial solutions at each node in the tree, which allows us to prune most of the suboptimal solutions early. Some criteria such as RCI_P need to be further decomposed; for more details see (*15*).

The basic idea of our algorithm builds on previously proposed algorithms for single-objective optimization on tree-structured networks (*34, 35*). Importantly, our algorithm approximates the Pareto frontier for multiple objectives. The details of the implementation of the algorithm used here are described in (*15*). Briefly, the algorithm applies a divide-and-conquer approach to prune dominated solutions more efficiently and a batching technique to cope with the large computational memory requirements of the multi-objective Pareto frontier. In practice, the algorithm can compute the exact Pareto frontier (ε=0) for two criteria within minutes and the approximate Pareto frontier (ε=0.25) for five criteria within a week. We observe that the solutions are generally very close to the actual Pareto frontier even when the error margin ε is relatively large.

2.4. Computing the Pareto-optimal frontier for six criteria

The runtime of our dynamic-programming based algorithm is polynomial for the number of dams but still exponential for the number of objectives, which means that both the runtime and the number of solutions increase dramatically as the number of objectives go up. For instance, for certain pairs of criteria (e.g. energy and greenhouse gas emissions), we are able to compute the exact Pareto frontier (ε=0) within 20 minutes (wall-clock time, 36 threads; ≈ 10 hours CPU time); for 5 criteria, we are able to run the algorithm for ε=0.4 in 17 hours (wall-clock time, 36 threads; ≈ 9.3 days CPU time).

When optimizing for all six criteria, however, we can only run for larger error margins such as ε=1.5 or ε=2.0, and the runtimes are 2 days and 7 hours (wall-clock time, 36 threads), respectively. Large error margins result in fewer solutions, with limited representation of the actual Pareto frontier. To provide more comprehensive representation, we complemented the approximate Pareto frontier with subsampled optimization results for all possible two and three criteria combinations with small error margins (ε=0.01 for two criteria and ε=0.1 for three criteria). Pareto-optimal solutions optimized for two and three objectives with lower error margins are generally Pareto-optimal when we consider all six objectives. While the Pareto frontier complemented with combinations of two and three criteria provides the guarantee associated with the simultaneous optimization with respect to six criteria (ε=1.5), it results in better coverage than the six-criteria Pareto frontier and affords a more desirable approximation of the actual Pareto frontier (fig. S2).

2.5. Interactive Pareto-frontier visualization

Visualizing the Pareto frontier on a two-dimensional space is straightforward when two criteria are considered. However, visualization becomes challenging for three or more criteria. As a supplement to this paper, we provide an interactive graphic (referred to as Amazon EcoVistas; (*18*)) for visualizing the Pareto frontier for proposed Amazon hydropower development based on the six criteria considered here. Our interactive graphic illustrates the Pareto frontier for each pair of energy and environmental criteria as well as all six criteria simultaneously, with the additional capability of setting ranges on the different criteria (fig. S3).

3. River network connectivity

Hydropower dams present physical barriers that can block the upstream-downstream movement of fish and other aquatic animals, impacting access to habitats and potentially impeding the ability of some organisms to complete their reproductive life cycle. While connectivity impacts may be most severe within the range of widely migrating diadromous fish (e.g. the Amazon goliath catfish *Brachyplatystoma rousseauxii (36)*), resident potamodromous fish species with localized migrations can also be affected as river network connectivity is impeded in the vicinity of dams. We implemented two metrics to represent network-wide reductions in river connectivity associated with dams based upon the 'dendritic connectivity index' (*37*). The dendritic connectivity index utilizes river segment length as the unit of currency, however, this approach fails to capture the widely differing amounts of aquatic habitat contained in large versus small rivers per unit length (*38*). Thus, we weighted dendritic connectivity indices by Strahler stream order, which has been shown to scale closely with amount of river habitat per unit length (*39*).

To represent localized connectivity impacts from hydropower dams, we calculated river order-weighted potamodromous connectivity, RCI_P:

(Eq. 1)

$$RCI_P = 100 * \sum_i \sum_j \frac{2^{r_i} l_i}{L^*} \frac{2^{r_j} l_j}{L^*} p_{ij}$$

where l_i is length for stream segment i weighted by 2 to the river order r ∈{1,2,3,…,12} as a proxy for river volume, $L^* = \sum_i 2^{r_i} l_i$ is the total river order weighted stream network length, and $p_{ij} \in \{0,1\}$ indicating the passability between river segments i and j. Scaled as a percentage where 100% indicates network-wide unimpeded connectivity, RCI_P characterizes the ability of fish to move unimpeded between randomly chosen segments in the river network (*37*).

RCI_P is relevant to connectivity impacts that would impede movement of both resident potamodromous and long-distance migrating diadromous taxa; however, optimizing for RCI_P is computationally expensive (*16*). We also implemented a simpler metric tailored to represent connectivity impacts to long distance migrating diadromous species, calculating river order weighted longitudinal connectivity for diadromous species, RCI_D, as:

(Eq. 2)

$$RCI_D = 100 * \frac{2^{r_1} l_1}{L^*}$$

where l_1 is length of the stream segment directly upstream of the river mouth to the first passability barrier with r and $L^* = \sum_i 2^{r_i} l_i$ defined as above. RCI_D characterizes the ability of fish to move unimpeded between the Amazon river mouth and any randomly chosen upstream segment in the river network.

4. Fish biodiversity

The Amazon Basin harbors the highest number of freshwater fish species in the world, many of which play critical ecological and socio-economic roles. To estimate the impacts of current and proposed dams on fish biodiversity we used information compiled by the Amazon Fish Project (https://www.amazon-fish.com/). This database compiled fish species distributions for 2,255 native freshwater fish species from 14,000 sites across the Amazon Basin, using online data (GBIF), museum specimens, published occurrences, and field expeditions at the resolution of the sub-basin level (*40*). To incorporate components of both endemism and species richness into a single metric that could be associated with each project, we adapted a weighted endemism index to account for both sub-basin and river discharge (*41*):

(Eq. 3)

$$E_D = \frac{\sum_{i=1}^{n} \frac{1}{range_i}}{Area_{sub-basin}} Q_D$$

Where E_D is fish weighted endemism at dam D, n is the number of fish species present in a sub-basin, $range_i$ is the number of sub-basins in which fish species i is present, $Area_{sub-basin}$ is the area of the focal sub-basin and Q_D is the discharge at the site of the dam D on the river network. The numerator in the fraction is the original weighted endemism formula, or a rarity-weighted index of fish species richness that counts species in inverse proportion to their range size, such that species with the smallest range size receive a higher value (*41*). This value is divided by sub-basin size to account for the positive relationship between basin area with fish species richness and endemism. Finally, to scale down our E_D index from the sub-basin to each individual project, we multiplied the index by the discharge along the reach of the project, which assumes that rivers with higher discharge tend to be more biodiverse (*42, 43*).

5. Flow regime alteration

Reservoir operations strongly modify the spatial and temporal patterns of downstream flows, affecting habitat integrity and ecosystem functions (*44-46*). We assessed downstream impacts on flow regime with a modified formulation of the Degree of Regulation (DOR) index (*47, 48*). For a given river reach, the DOR gives the proportion of the annual flow that can be withheld by upstream reservoirs, thus providing an approximation of the cumulative impacts of all upstream dams on downstream flow regimes.

The conventional formulation of DOR does not incorporate potential attenuation associated with the relative location of upstream reservoirs (e.g., the number and size of reservoirs, proximity of the river reach to the upstream reservoirs, or if the reservoirs are located in sequence in the same branch or in different branches). To incorporate the fact that flow alterations tend to be attenuated as one moves downstream of a dam, we included the ratio between flow at the dam site (Q_d) and the river reach (Q_r) as a weighting factor. At a given river reach *r*, DOR was then calculated as:

(Eq. 4)

$$DoRw_r = \sum_{d \in D} \frac{Q_d V_d}{Q_r^2} * 100[\%]$$

Where *d* is the sub-index referring to a given reservoir, *D* is the sub-index referring to the subset of reservoirs upstream of reach *r*, V is the total storage volume of a reservoir (m^3), and Q is the average annual discharge ($m^3\ yr^{-1}$). Long-term average discharge was estimated with a statistical scaling model based on the correlation between cumulative upstream precipitation from the MSWEP v1.1 dataset (*49*) and observed discharges at 304 gauges (R^2=0.96). For each dam location, the discharges estimated from the empirical model were further validated with a large-scale rainfall-runoff model (Supplementary Text 2). DOR_w values at reservoir locations were highly variable (range: 0% to 392%), ranging from projects with no capacity to withhold water to reservoirs with high potential to alter natural flow regimes.

To run the optimization, for each portfolio of dams *S*, we calculated the sum of DOR_w over the length of the entire river network to obtain a single combined estimate of the spatial extent of the basin affected by dam operations. We take advantage of the linearity of the criterion to streamline the computation. To quantify the overall contribution to downstream impact of each dam, we define $C_{DoR}(d)$ as:

(Eq. 5)

$$C_{DoR}(d) = \left(\sum_{r \epsilon R} \frac{Q_d V_d}{Q_r^2} l_r \right)$$

Where R is the subset of river reaches in the entire network, and l_r the length of reach r. For a given portfolio of dams S, integrating the DOR_w values over the river network is equivalent to summing the C_{DoR} in the portfolio, such that minimizing the DOR criterion is the same as minimizing the sum of C_{DoR} of dams in the portfolio:

(Eq. 6)

$$\sum_{r \epsilon R} DoRw_r\,(S) \cdot l_r = \sum_{d \in \boldsymbol{S}} C_{DoR}(d)$$

6. Sediment transport

The Amazon is one of the few remaining rivers where natural sediment flows predominate and determine multiple physical and ecological characteristics of rivers and their associated ecosystems, including nutrient delivery, thermal regime, and geomorphology (*50, 51*). Artificial reservoirs entrap transported sediment and associated nutrients and reduce delivery to downstream freshwater and coastal marine environments. Deficits in sediment loads can be responsible for various downstream impacts, including erosion and subsidence of river deltas (*52*), progressive changes in river morphology (*53*), and depletion of nutrients essential for primary production (*54*).

For a given portfolio of hydropower sites, our desired objective was to minimize the total amount of sediment trapped basin wide. We first estimated the percentage of sediment trapped of each reservoir (trapping efficiency, TE), using the lower boundary of Brune's empirical curve (*55*), which is based on the ratio of reservoir volume (m^3) and inflowing discharge ($m^3\ yr^{-1}$). We then assessed the cumulative effect associated to relative locations of reservoirs, as upstream reservoirs may reduce sediment input to downstream reservoirs.

We developed a model to estimate total sediment transport across the river network based on sediment balance of production processes (slope and channel erosion) and deposition (bank overflow) at a given river reach, r:

(Eq. 7)

$$T_r = \sum_{r \in U_T} S_r = \lambda_1\Big(\sum_{r \in U_T} ESPh_r \cdot l_r\Big) + \lambda_2\Big(\sum_{r \in U_T} ESPl_r \cdot l_r\Big) - \lambda_3\Big(\sum_{r \in U_T} W \cdot l_r\Big)$$

Where *ESP* is the regional proxy of the sediment yield, calculated as the product of standardized (0 to 1) average reach elevation, average reach slope (*48*) and annual precipitation (*49*). Sediment yield proxy is partitioned for reaches above 500 m of elevation (*ESPh*) or below (*ESPl*), to differentiate active tectonic uplift and subsidence that have been suggested to control long-term sedimentation and erosional process in the sub-Andean region. Regional proxy of upstream sediment deposition, *W*, is the map of wetland extent, vegetation type, and dual-season flooding state of the entire lowland Amazon Basin (*56*), re-classified as: wetland =0 if not wetland, wetland=1 otherwise. l is length. To ensure that our results preserve mass balance, we also constrained the model so the total amount of sediment in every river reach should be above 0. Model parameters (λ) were calibrated to fit reported data at 66 sediment gauges located across the basin ($R^2 = 0.92$).

7. Greenhouse gas emissions

The construction of reservoirs generally results in net increases of greenhouse gas emissions—principally methane—to the atmosphere (*57, 58*). Reservoirs can thus be considered anthropogenic sources of greenhouse gases. In fact, some proposed Amazon dams with large reservoir areas relative to electricity generation capacity may emit more greenhouse gases per unit electricity generated than conventional fossil fuel power plants (*13*). It is therefore critical to minimize greenhouse gas emissions from reservoirs as hydropower dam construction proliferates across the basin. We used net greenhouse gas emission estimates available for the dams in our database (*13*). This approach combines project-specific data on reservoir surface area and installed capacity from our Amazon dams with published observations of carbon dioxide and methane emissions reported for tropical and subtropical reservoirs to calculate likely ranges of emissions per unit electricity generated for all existing and proposed Amazon dams (*57, 58*). The ratio of installed capacity to reservoir surface area, commonly known as power density, is a key determinant of emissions per unit electricity generated (*59-61*). Our emission estimates are for a 100-year time horizon, and we transform methane emissions into carbon dioxide equivalents (CO_2eq) considering a global warming potential of 34 for methane (*62*).

Supplementary Text 1

Visualizing the Pareto frontier is in itself a major challenge. Indeed, simultaneous consideration of three or more criteria adds considerable complexity to interpreting optimization outcomes, given the inherent limitations of human cognition to visualizing high-dimensional spaces. This is further compounded with the fact that our methods have the power to generate the unconstrained Pareto frontier for the full range of criteria at a fine grain, which translates into a very large number of Pareto optimal solutions—in the millions or even higher. To visualize this high-dimensional Pareto frontier we provide several representations. While the main text includes several user-friendly 2-D representations, we stress that they misrepresent the high-dimensional capabilities of our framework that can truly reason and optimize the Pareto frontier at much higher dimensions. Therefore, we also developed 6-D parallel plot representations to capture all criteria simultaneously. In addition to facilitate navigating this high-dimensional Pareto frontier, we developed Amazon EcoVistas (*18*), an interactive graphical user interface bringing together a range of perspectives: (1) the simple 2-D Pareto frontier optimizing energy with respect to each environmental criterion individually (as in Fig 2A); (2) the comparative 2-D Pareto frontier in which the standard 2-D Pareto frontier optimizing energy with respect to another criterion X is compared against a frontier obtained for energy against criterion X but when optimizing energy with respect to a criterion Y. This representation demonstrates the suboptimality of solutions for criterion X when optimizing with respect to criterion Y, as in Fig 3C for energy versus sediment (X) and different instantiations of Y; (3) the Pareto frontier simultaneously optimized with respect to 6 criteria, projected as 2-D, i.e., energy vs. another criterion (figure not shown in manuscript); (4) 6-D Pareto frontier using a 6-D parallel plot, in parallel line corresponding to a criterion, with the capability of constraining the range for each criterion, which results in elimination of solutions outside the selected ranges. This capability is useful for further refining the Pareto frontier based on constraints with respect to each criterion (e.g., at least a certain value or no more than a certain value, or within a certain range).

Supplementary Text 2

Annual average discharge was estimated with a scaling model procedure based on the correlation between discharge of 304 in-situ Amazon Basin gauges and daily precipitation from the MSWEP v1.1 dataset (*49*). The location and specific details about these gauges are summarized in fig S4 and table S2.

Fig S5A presents the empirical model adjustment to precipitation estimates, and fig. S5B the comparison between adjusted and observed streamflow. We validated discharge estimates for the location of all 509 dams in our database with MGB, a continental-scale hydrological model (*63*). The comparison of discharges estimated using both methods show a satisfactory agreement between them (fig S5C). There is some disagreement between dams located at very downstream reaches (i.e. large drainage areas), which may be related to floodplain attenuation effects that are not considered in the scaling method.

Supplementary Figures

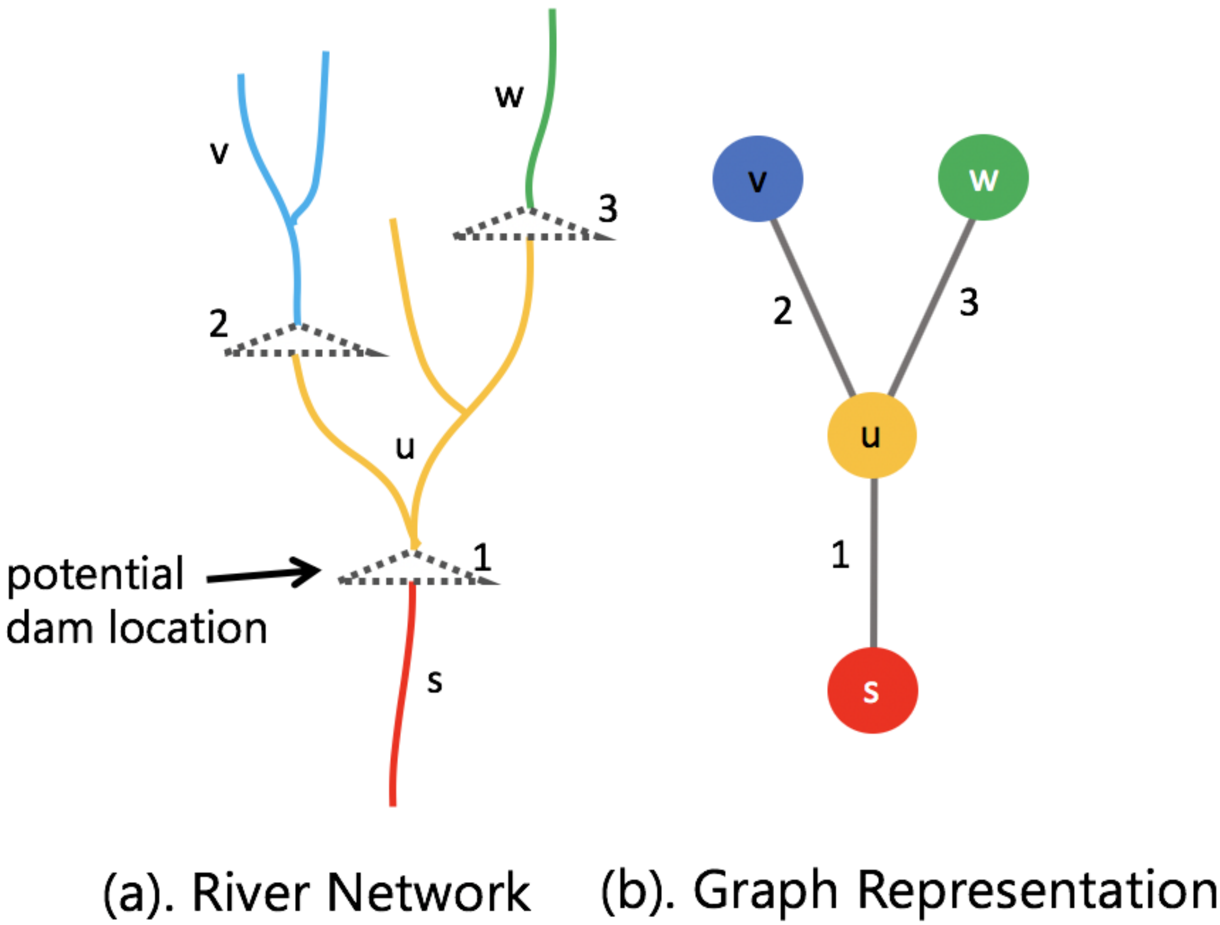

Fig. S1. Converting a river network (left) into a more compact directed rooted tree (right), where s represents the root of the river network. Each contiguous region of the river network (represented by different colors, and labeled s, u, v, w) is represented as a hypernode (labeled with the corresponding letter, s, u, v, w) in the tree network. Each potential dam location (shown in the left as triangles and labeled 1, 2, 3) is represented as an edge in the directed rooted tree.

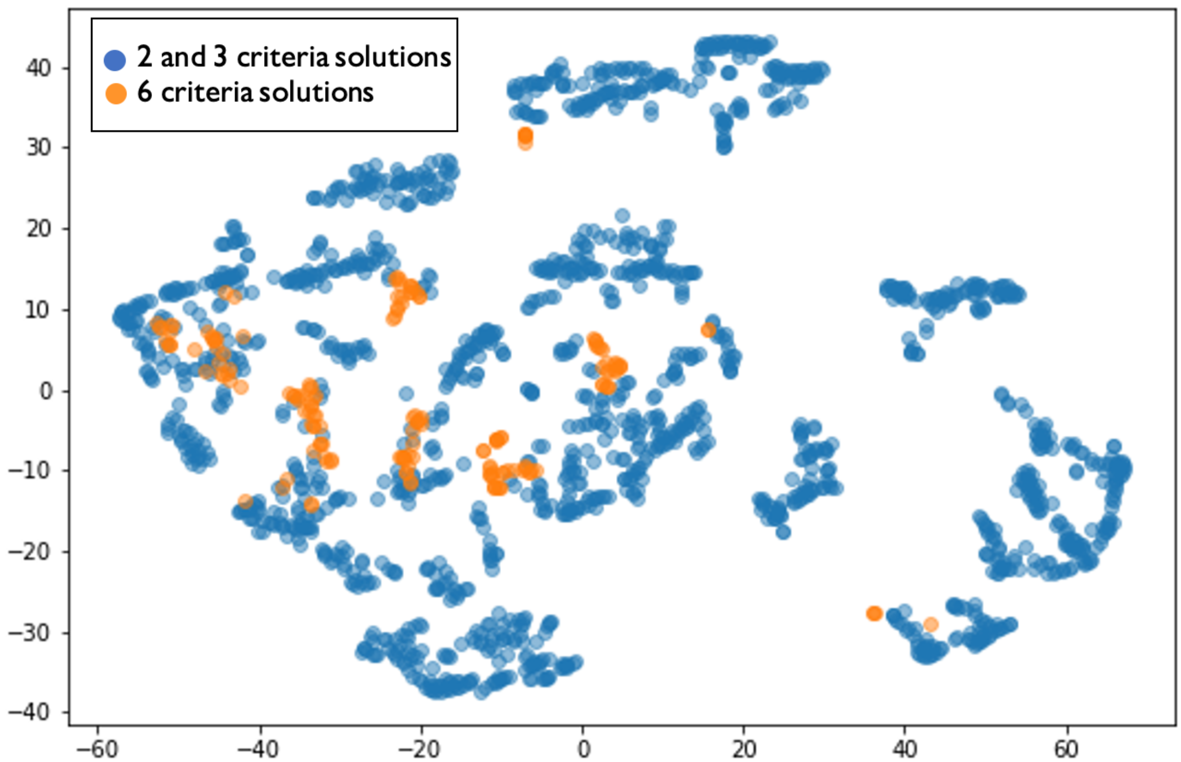

Fig. S2. Non-linear dimension reduction using t-distributed stochastic neighbor embedding (t-SNE) for showing 2-dimensional projection of 6-dimensional solutions. The approximate Pareto frontier is complemented with subsampled optimization results for all possible two and three criteria combinations with small error margins (ε=0.01 for two criteria and ε=0.1 for three criteria). While the Pareto frontier complemented with combinations of two and three criteria only provides the guarantee associated with simultaneous optimization of six criteria (ε=1.5), the figure shows there is better coverage than afforded by the 6-criteria Pareto frontier alone.

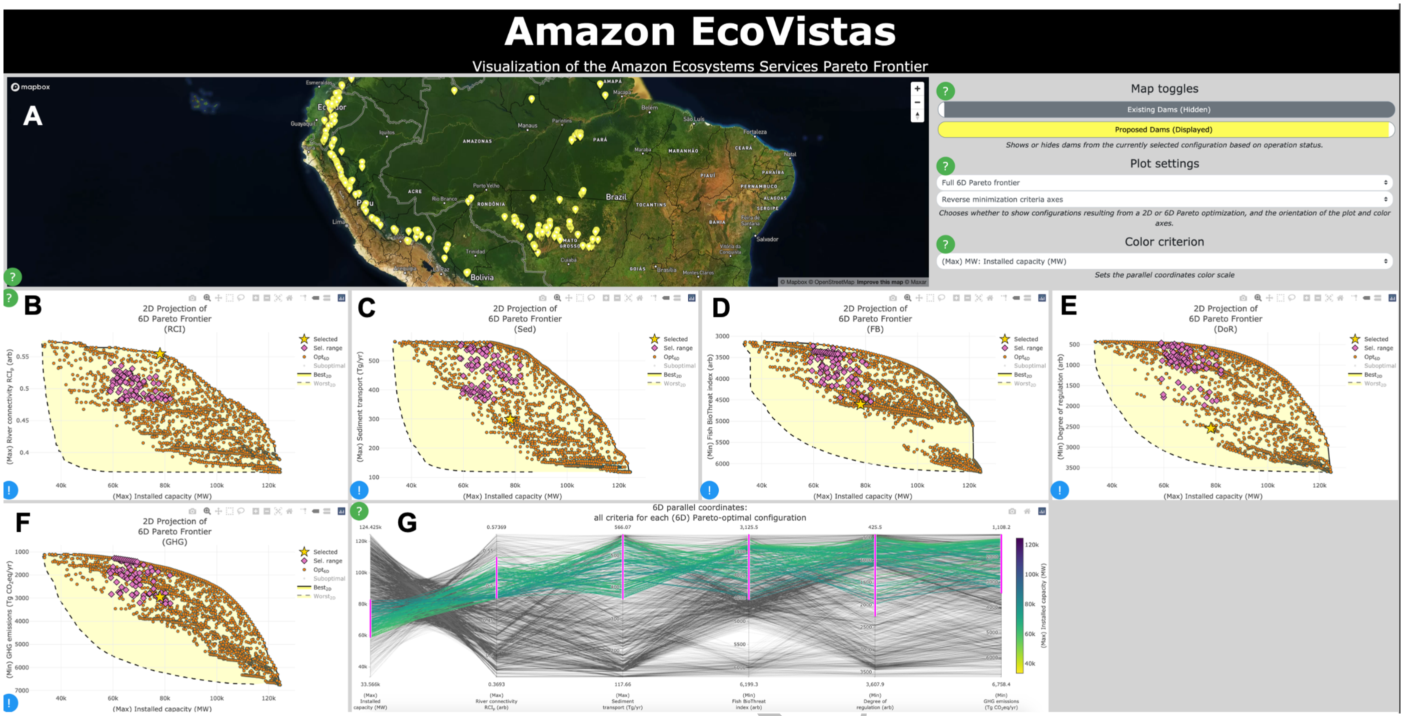

Fig. S3. Snapshot of Amazon EcoVistas, (https://www.cs.cornell.edu/gomes/udiscoverit/amazon-ecovistas/), an interactive graphic for visualizing Pareto frontiers. Amazon EcoVistas provides three types of visualizations. The first one is an interactive map (**a**) showing the locations of dams contained in a given solution selected by clicking a specific point (yellow star) in the 2-D scatter plots (**b-f**). The 2-D scatter plots (**b-f**) show criterion-specific outcomes for each solution in the 6-D Pareto frontier, illustrating the tradeoffs for each pair of energy and environmental criteria when all criteria are considered together. The magenta diamonds in **b-f** are solutions selected using the parallel coordinate plot (shown as colored lines in **g**); the orange dots are the remaining unselected solutions in the 6-D Pareto frontier. In the parallel coordinate plot in **g**, each coordinate corresponds to the value of a criterion, and each zigzag line connecting different values on the coordinates corresponds to a single solution. Constraints can be added on each criterion (shown as pink lines on the coordinates) and only the solutions that satisfy the constraints will be shown in color.

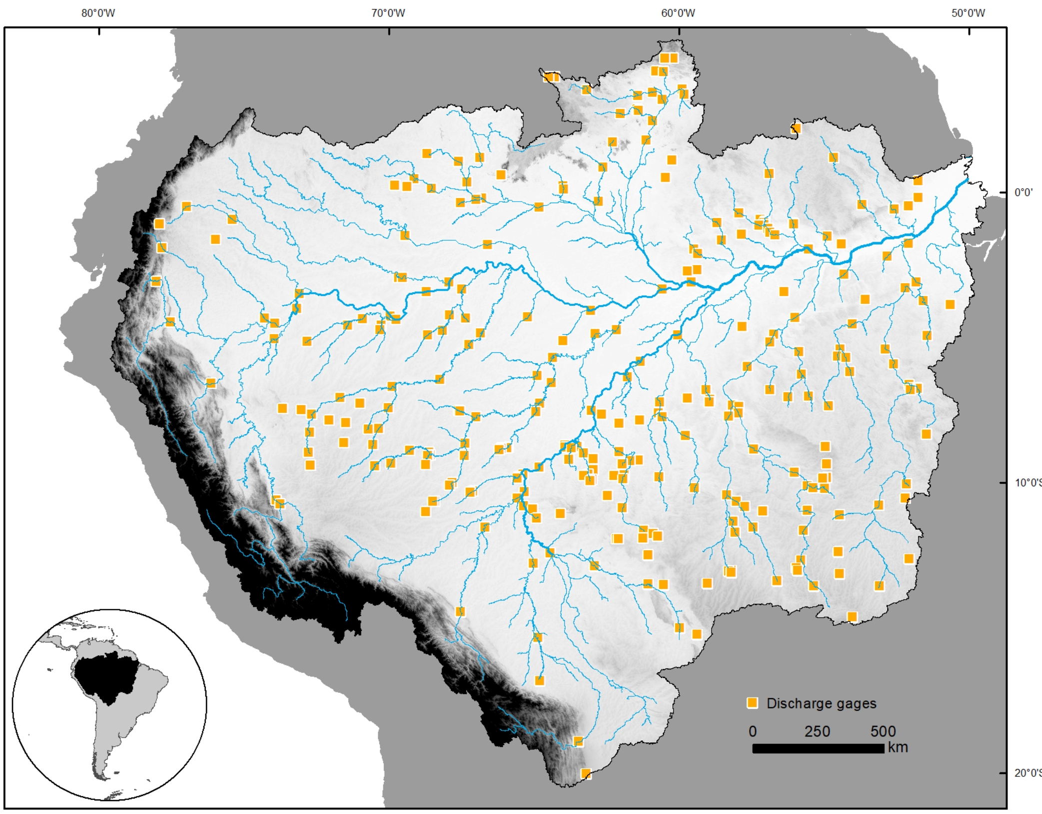

Fig. S4. Location of gauges used in the discharge estimations (n = 304).

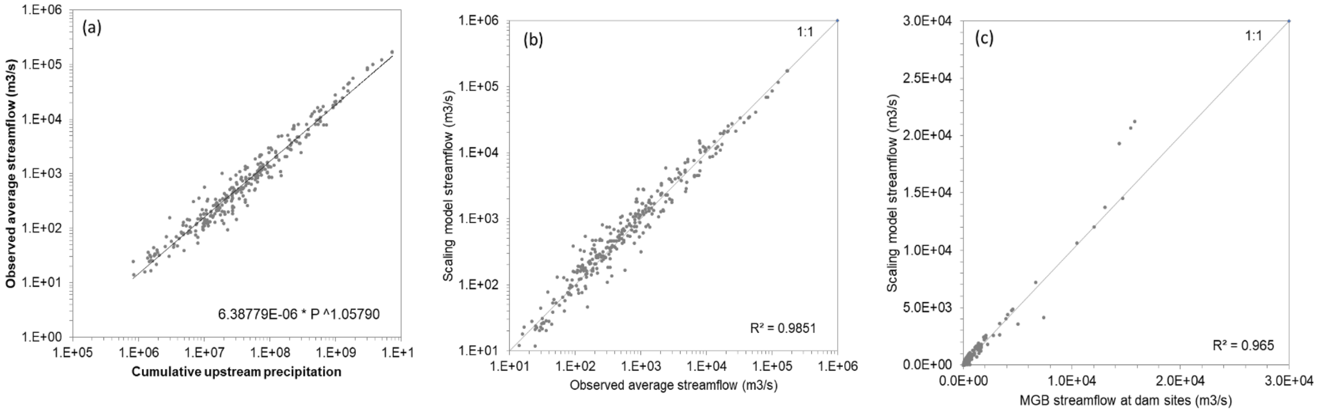

Fig. S5. (a) Scaling model adjustment between observed discharge and precipitation. (b) Scaling model estimates of discharges. (c) Scaling model validation with MGB hydrological model estimates for all 509 dam sites in our database.

Supplementary Tables

Table S1. Number and total installed capacity of existing and proposed hydropower dams per major sub-basin in the Amazon. Major sub-basins are defined as all tributary basins >100,000 km^2 whose main stems flow into the Amazon River as well as small tributary basins draining directly into the Amazon main stem.

		Existing dams		Proposed dams	
Major basin	**Basin area (km^2)**	**Number**	**Total capacity (MW)**	**Number**	**Total capacity (MW)**
Tapajós	494,743	25	3,239	144	25,699
Marañón	363,839	32	3,335	62	27,843
Madeira	1,323,438	60	9,822	52	18,378
Ucayali	354,660	18	2,280	36	12,160
Napo	101,323	8	1,665	16	2,592
Jari	134,745	2	614	15	3,118
Xingu	508,962	8	11,332	11	78
Negro	719,574	1	5	5	1,052
Purus	369,741	0	0	5	125
Abacaxis	127,670	0	0	3	170
Japurá - Caquetá	254,001	0	0	1	665
Uatumã	73,611	3	285	1	8
Curuá-Una	30,803	1	30	0	0

Table S2. Number and sources of gages used in our discharge estimations.

Source/Country	Bolivia	Brazil	Colombia	Ecuador	Guyana	Peru	Venezuela	Total
Armijos et al. 2013 (*64*)				1		8		9
Coe et al. 2008 (*65*)		5						5
Laraque et al. 2007 (*66*)				3				3
Moquet et al. 2011 (*67*)				2				2
Ovando et al. 2016 (*68*)	2							2
Pepin et al. 2013 (*69*)	2					1		3
Tucker-Lima et al. 2016 (*70*)	5	268	1		1		1	276
Vauchel et al. 2017 (*71*)	4							4
Total	13	273	1	6	1	9	1	304